Insertion of a SNS-specific tetrapeptide in S3–S4 linker of D4 accelerates recovery from inactivation of skeletal muscle voltage-gated Na channel μ1 in HEK293 cells

S.D. Dib-Hajj[a,b], K. Ishikawa[a,b], T.R. Cummins[a,b], S.G. Waxman[a,b,*]

[a]*Department of Neurology, Yale University School of Medicine, 333 Cedar Street, New Haven, CT 06510, USA*
[b]*Neuroscience Research Center, VA Medical Center, West Haven, CT 06516, USA*

Received 23 July 1997

Abstract **Na channel subunits αSNS (PN3) and αμ1(SkM1) produce slowly inactivating/TTX-resistant and rapidly inactivating/TTX-sensitive currents, respectively. αSNS (PN3) current recovers from inactivation (reprimes) rapidly. Sequence alignment identified the tetrapeptide SLEN, in the S3–S4 linker of D4, as αSNS-specific. To determine whether SLEN endows Na channels with slow kinetics and/or rapid repriming, we analyzed the transient Na current produced by a chimera μ1SLEN in HEK293 cells. Neither kinetics nor voltage dependence of activation and inactivation was affected. However, repriming was twice as fast as in the wild type at −100 mV. This suggests that SLEN may contribute to the rapid repriming of TTX-resistant Na current.**

Key words: Voltage dependence; Na current kinetics; Channel repriming; TTX

1. Introduction

Voltage-gated sodium channels consist of a large, 260 kDa, pore-forming, α-subunit and one or more auxiliary β-subunits [1,2]. The α-subunit polypeptide chain consists of four homologous domains (D1–4), each with six predicted transmembrane segments (S1–6) joined by cytoplasmic and extracellular loops [1]. Except for the loop joining domains III and IV (D3–4 linker), which contains the conserved inactivation particle [3,4], the amino acid sequences of these loops and the N- and C-termini are less conserved than those of the transmembrane segments [5,6]. The amphipathic S4 segment of each domain with its positively charged residues is thought to be the voltage sensor [1,7,8]. Two types of Na currents are produced by these α-subunits: slow inactivating, TTX-resistant (slow/TTX-R) and fast inactivating, TTX-sensitive (fast/TTX-S) [1]. The α-subunits from human and rat skeletal muscle, SkM1 and μ1, respectively, produce fast/TTX-S Na currents [9–12]. Recently, two groups have cloned an α-subunit SNS (PN3) which produces a slow/TTX-R Na current when expressed in *Xenopus* oocytes [13,14]. Studies on dorsal root ganglion (DRG) neurons have provided strong evidence that SNS produces the slow/TTX-R current in these cells [15,16].

A number of cDNAs encoding α-subunits have been cloned [6]. Amino acid residues that are proposed to play specific roles such as voltage sensors, inactivation particle, ion selectivity filters and toxin binding sites are conserved in these subunits [5,6,17]. In K channels, activation involves the movement of the N-terminal portion of S4 into the extracellular space from a position inside the membrane at rest [7]. The TTX-R current in C-type DRG neurons, which appears to be encoded by SNS [13,18], is characterized by slow activation and inactivation kinetics [19–21] and by rapid recovery from inactivation (repriming) [16,21]. We reasoned that sequence variation in or around the voltage sensor, S4, may contribute to the slow kinetics and rapid repriming of the SNS/PN3 current. Alignment of the amino acid sequence of the linker joining S3 and S4 of domain 4 (D4S3–S4) and D4S4 of SNS shows a non-conservative substitution of an invariant amino acid residue followed by a tripeptide insertion compared to the rest of the mammalian α-subunits. This difference is intriguing because this region appears to be crucial for coupling activation to fast inactivation [22,23], slowing down inactivation and accelerating repriming of SkM1 [24,25]. Therefore we constructed a chimera μ1 construct carrying the SNS-specific tetrapeptide at the analogous position in the D4S3-S4 linker and analyzed the Na current produced by this chimera in HEK293 cells.

2. Materials and methods

2.1. Plasmid construction

The plasmid μ1-RBG4 [10] was used to generate a chimera construct for this study. One wild type primer pair (F1 and R1) and one mutagenic pair (M1 and M2) were used to introduce the insertion into the S3-S4 linker. Wild type forward primer F1 (5′-CGGTGGTCAACAACAAGTCCG-3′) and reverse primer R1 (5′-ATGCCGAAGATCGAGTAGATG-3′) correspond to nucleotides 4030–4050 and 4910–4930, respectively. Mutagenic primers M1 (5′-CACAAAGTTTTCCAGTGATTTCTGTATCAAGTCAGAGAG-3′) and M2 (5′-CAGAAATCACTGGAAAACTTTGTGTCACCCACGCTGTTC-3′) correspond to nucleotides 4725–4754 and 4740–4770, respectively, plus the extra 12 nucleotides (underlined). PCR was performed in 60 μl volume using 3 μM of each primer and 1.75 units of Expand Long Template DNA polymerase enzyme mixture in buffer 3 (Boehringer Mannheim). Amplification was carried out in two stages for a total of 30 cycles, as previously described [26], using a programmable thermal cycler (PTC-100, MJ Research, Cambridge, MA).

A PCR-based mutagenesis and cloning method [27] was used to produce μ1SLEN-RBG4 plasmid. Two separate PCR reactions were performed using 10 ng μ1-RBG4 as template and F1/M1 and M2/R1 primer pairs, respectively. The two PCR products were band isolated and used as a mixed template for PCR using primer pair F1/R1. The resulting PCR product, exchanged Y^{1433} with the tetrapeptide SLEN in the S3–S4 linker, was cloned using pCR-Script vector (Stratagene) to produce plasmid pSLEN. The insert in pSLEN was sequenced to confirm the nucleotide changes. Plasmid μ1SLEN-RBG4 was constructed by replacing the unique *AccI*/*Bsp*EI fragment, which corresponds to nucleotides 4067–4836, from the wild type construct μ1-RBG4 with that of the mutant construct pSLEN.

*Correspondence: Fax: (1) (203) 785-7826.
E-mail: Stephen.Waxman@yale.edu

PII S0014-5793(97)01154-X

2.2. Expression system

The μ1-RBG4 and μ1SLEN-RBG4 constructs were cotransfected into HEK293 cells with a fluorescent reporter plasmid (pGreen Lantern-1 Gibco) using the calcium-phosphate precipitation technique [10]. HEK293 cells were grown in high-glucose DMEM (Gibco) supplemented with 10% fetal calf serum (FCS; Gibco). After 48 h, cells with green fluorescence were selected for recording.

2.3. Whole-cell recordings

Whole-cell patch-clamp recordings were conducted at room temperature (21°C) using an EPC-9 amplifier. Data were acquired on a Macintosh Quadra 950 using the Pulse program (v. 7.52, HEKA, Germany). Fire-polished electrodes (0.8–1.5 MΩ) were fabricated from 1.65-mm capillary glass (WPI) using a Sutter P-87 puller. Cells were not considered for analysis if initial seal resistance was <5 GΩ, they had high leakage currents (holding current >0.1 nA at -80 mV), membrane blebs, or an access resistance >5 MΩ. Access resistance (3 ± 1 mV, mean ± S.D., $n=42$) was monitored throughout the experiment and data were not used if resistance changes occurred. Voltage errors were minimized using 80% series resistance compensation and the capacitance artifact was cancelled using the amplifier computer-controlled. For comparisons of the voltage dependence of activation and inactivation, only cells with a maximum voltage error of <10 mV after compensation were used. The voltage error was 4 ± 3 mV for μ1-RBG4 ($n=16$) and 5 ± 2 mV for μ1SLEN-RBG4 ($n=14$). Linear leak subtraction was used for all voltage clamp recordings. Membrane currents were filtered at 5 kHz and sampled at 20 kHz. The pipette solution contained: 140 mM CsF, 2 mM $MgCl_2$, 1 mM EGTA, and 10 mM Na-HEPES (pH 7.3). The standard bathing solution was 140 mM NaCl, 3 mM KCl, 2 mM $MgCl_2$, 1 mM $CaCl_2$, 10 mM HEPES, and 10 mM glucose (pH 7.3). Data were not corrected for liquid junction potentials which were <5 mV. The osmolarity of all solutions was adjusted to 310 mOsm.

2.4. Data analysis

Data were analyzed using Pulsefit (v. 7.52) or custom software developed by T.R. Cummins. Unpaired *t*-test analysis (using the Systat program) required $P<0.05$ for significance. Analysis results are expressed as mean ± standard deviation. The curves in the figures are drawn to guide the eye unless otherwise noted.

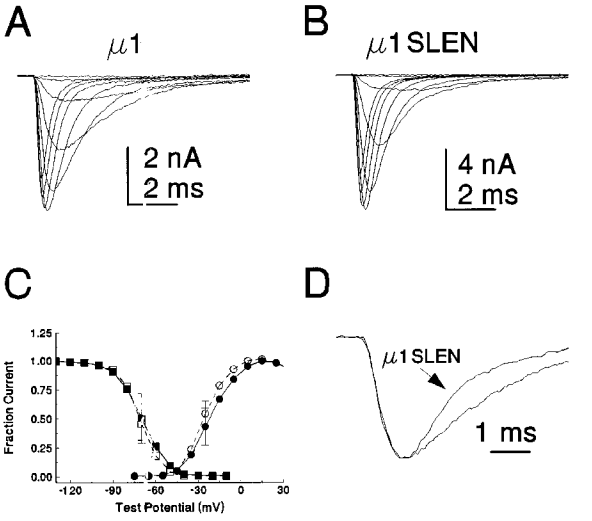

Fig. 2. Comparison of μ1 and μ1SLEN currents in HEK293 cells. A, B: Family of traces from representative HEK293 cells expressing either μ1 (A) or μ1SLEN (B) channels. The currents were elicited by 40 ms test pulses to various potentials from −65 to 10 mV. Cells were held at −100 mV. C: The activation (circles) and steady-state fast inactivation (squares) curves for μ1 (filled symbols; $n=16$) and μ1SLEN (open symbols; $n=14$) channels. Steady-state fast inactivation was measured with 500 ms inactivating prepulses. Cells were held at prepulse potentials over the range of −130 to +10 mV prior to a test pulse to −10 mV for 20 ms. Current is plotted as a fraction of peak current. D: Representative traces from cells expressing μ1 and μ1SLEN channels. Cells were held at −100 mV and stepped to −35 mV for 20 ms. No difference was observed in the rate of activation, but the μ1SLEN current inactivated slightly faster than μ1 current.

```
GSLLFSAILKSLENYFSPTLFRVIRLARIGRILRLIRAAKGIRTLL  rSNS
ASLLFSAILKSLESYFSPTFFRVIRLARIGRILRLIRAAKGIRTLL  mSNS
GTVLSDIIQKY---FFSPTLFRVIRLARIGRILRLIRGAKGIRTLL  rH1
GLALSDLIQKY---FVSPTLFRVIRLARIGRVLRLIRGAKGIRTLL  rμ1
GMFLAELIEKY---FVSPTLFRVIRLARIGRILRLIKGAKGIRTLL  rαI
GMFLAELIEKY---FVSPTLFRVIRLARIGRILRLIKGAKGIRTLL  rαII
GMFLAELIEKY---FVSPTLFRVIRLARIGRILRLIKGAKGIRTLL  rαIII
GMFLADIIEKY---FVSPTLFRVIRLARIGRILRLIKGAKGIRTLL  rαVI
GMFLAEMIEKY---FVSPTLFRVIRLARIGRILRLIKGAKGIRTLL  rPN1
GMFLAEMIETY---FVSPTLFRVIRLARIGRILRLIKGAKGIRTLL  NaS
GMFLADMIETY---FVSPTLFRVIRLARIGRILRLVKGAKGIRTLL  hNE
GLCLPMTVGSY---LVPPSLVQLILLSRIIHMLRLGKGPKVFHNLM  hNav2.1
GLLLPLTIGQY---FVPPSLVQLILLSRVIHILRPGKGPKVFHDLM  mNav2.3
GLLLPLSIGQY---FVPPSLVQLLLLSRIIHVLRPGKGPKVFHDLM  rNaG
 S3                    S4
GSLLFSAILKSLENYFSPTLFRVIRLARIGRILRLIRAAKGIRTLL  rSNS
GLALSDLIQKSLENFVSPTLFRVIRLARIGRVLRLIRGAKGIRTLL  rμ1SLEN
GLALSDLIQKY---FVSPTLFRVIRLARIGRVLRLIRGAKGIRTLL  rμ1
   *    123   4567890
```

Fig. 1. Parsimonious alignment of select domain 4 sequences of mammalian α-subunits: S3 (terminal octatapeptide), S3–S4 linker and S4. Sequences of known mammalian α-subunit sequences were aligned to minimize number of gaps. The asterisk denotes L^{1433} of huSkM1 whose mutation induces changes in inactivation and recovery from inactivation of the skeletal Na channel [24,25]. The terminal octatapeptide of D4S3 and all of D4S4 are delineated by thick lines. The invariant Y residue at position 3 of the linker of rμ1 is changed to S followed by an insertion of the tripeptide LEN. Only one (rat) sequence is shown when the respective cognates from other species are identical or when the same subunit was reported by multiple groups. Accession numbers are: SNS: X92184 (rat); PN3: U53833 (rat, identical to SNS); mSNS:Y09108 (mouse); rH1: M27902 (rat); hSkM2: M77235 (human, rH1 cognate); rμ1: M26643 (rat); huSkM1: M26643 (human, rμ1 cognate); hoSkM1: U25990 (horse, rμ1 cognate); rαI: X03638 (rat); rαII: X03639 (rat); huαII: 476881 (human, rαII cognate); rαIII: Y00766 (rat); rαVI: L39018 (rat); mαVI: U26707 (mouse, rαVI); rPN1: U79568 (rat); hNE-Na: X82835 (human, rPN1 cognate); NaS: U35238 (rabbit, rPN1 cognate); $hNa_v2.1$: M91556 (human); $mNa_v2.3$: L36179 (mouse); NaG: M965778 (rat); and SCL-11:Y09164 (rat, full length NaG-like).

3. Results and discussion

All mammalian channels of subfamily 1 [28] including SNS (PN3) share a nearly identical D4S4 segment (Fig. 1), consistent with the role this segment plays as a voltage sensor [7,8]. The exceptions are the three atypical sodium channels of subfamily 2 [28] whose current properties are not known since none has been successfully studied in an expression system [28–30]. The remarkable conservation of the S4 sequence, including all the charged residues (Fig. 1), suggests that this segment does not confer slow activation and inactivation and rapid repriming on the Na current produced by SNS.

The D4S3-S4 linker of SNS/PN3 is remarkably divergent from other subfamily 1 channels (Fig. 1). The linker is longer (13 amino acid residues instead of 10) and contains significant amino acid changes. Compared to channels other than muscle (cardiac and skeletal) and the atypical channels, a non-conservative change, glutamic acid (E) to leucine (L), occurs at position 1; the muscle and atypical channels have glutamine (Q) and glycine (G) residues, respectively. An invariant tyrosine (Y) residue at position 3 is replaced with serine (S) and the tripeptide leucine-glutamic acid-asparagine/serine (LEN/S) insertion follows. Other more conservative changes, phenylalanine (F) to tyrosine (Y) and valine (V) to phenylalanine (F), occur at positions 4 and 5, respectively. The V to F substitution is also present in the cardiac channel (Fig. 1).

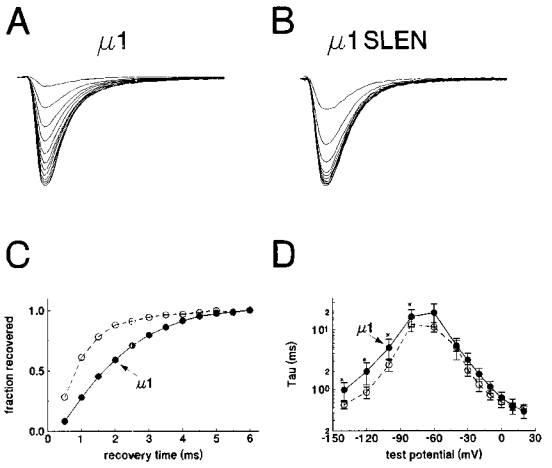

Fig. 3. Recovery from fast inactivation is quicker for μ1SLEN currents than μ1 currents. A, B: Family of traces from cells expressing μ1 (A) and μ1SLEN (B) currents showing the rate of recovery from inactivation. The cells were prepulsed to −10 mV for 20 ms to inactivate all of the current, then brought back to −120 mV for increasing recovery durations prior to the test pulse to 0 mV. The recovery time at −120 mV ranged from 0.5 ms to 6 ms in increments of 0.5 ms. C: Recovery from inactivation time course for the μ1 (filled circles) and μ1SLEN (open circles) currents shown in (A,B). The μ1SLEN current recovers about twice as fast as the μ1 current. D: Comparison of μ1 ($n=6$) and μ1SLEN ($n=7$) inactivation kinetics as a function of voltage. Time constants were measured from the rate of decay (test potentials between −50 and 20 mV) or from the time course for the recovery from fast inactivation (test potentials between −150 and −50 mV).

We reasoned that this dramatic sequence difference in this linker may impact the kinetics of D4S4 and/or D4S3 conformational transitions, hence the current properties. We tested the possibility that this difference may contribute to the slow kinetics and/or rapid repriming of the SNS/PN3 current by characterizing the current properties of the μ1SLEN chimera in HEK293 cells.

Sodium currents were recorded from cells expressing either the μ1 (Fig. 2A) or the μ1SLEN channels (Fig. 2B). The peak current density was slightly larger in cells expressing μ1SLEN channels (728 ± 616 pA/pF, $n=20$) than in cells expressing μ1 channels (515 ± 517 pA/pF, $n=23$).

In DRG neurons, the TTX-R current activates at potentials that are 10–15 mV more depolarized than the TTX-S current [16,19,21,31]. Activation kinetics are also much slower for TTX-R currents than for TTX-S neuronal or skeletal muscle sodium currents. Kostyuk et al. [19] estimated that the time constant of activation is about 5–10 times slower for the TTX-R current than for TTX-S currents. The SLEN mutation, however, did not alter activation of μ1 channels. We found no difference in the voltage dependence of activation (Fig. 2C) or in the rate of activation (Fig. 2D). At −35 mV, the time constant for activation was 0.46 ± 0.05 ms ($n=11$) for μ1 and 0.43 ± 0.07 ms ($n=15$) for μ1SLEN currents.

TTX-R currents in DRG neurons also exhibit very different inactivation properties from TTX-S currents. The midpoint for steady-state inactivation (V_h) is near −35 mV, which is about 30 mV more depolarized than what is typically observed for most TTX-S currents, including μ1. The V_h for recombinant SNS channels expressed in oocytes, which are TTX-R, is near −30 mV [13]. However, no difference was observed in the voltage dependence of steady-state inactivation of μ1SLEN and μ1 currents (Fig. 2C). The rate for the development of inactivation was, if anything, slightly faster for μ1SLEN than for μ1 currents (Fig. 2D). At −35 mV the time constant for fast inactivation was 3.5 ± 1.0 ms ($n=11$) for μ1 and 2.7 ± 0.8 ms ($n=15$) for μ1SLEN currents.

Repriming is much quicker for TTX-R currents in DRG neurons than for TTX-S currents [16,21]. At −120 mV, μ1SLEN currents reprimed faster than did μ1 currents (Fig. 3A,B,C). The time constant for repriming was about twice as fast for μ1SLEN currents ($\tau=0.9\pm0.2$ ms, $n=11$) than for μ1 currents ($\tau=2.0\pm0.8$ ms, $n=9$), and this difference was highly significant ($P<0.001$). The rate of repriming was faster for μ1SLEN currents at all voltages tested (Fig. 3D).

These data indicate that the D4S3–S4 linker is an important determinant of repriming in sodium channels. The accelerated rate of repriming may indicate a SLEN-induced destabilization of the closed-inactivated state of the channel, perhaps by affecting the conformational transition of D4S3 and/or D4S4. This is consistent with an earlier study [25] which concluded that D4S3 was an important determinant for repriming and suggested that repriming may be influenced by interaction between D4S3 and D4S4, such as sliding past each other. Notably, the SLEN insertion did not slow the onset of inactivation or shift steady-state inactivation to more depolarized potentials. Thus the alteration of an otherwise highly conserved D4S3–S4 linker appears to focally effect repriming. This observation may indicate a lower tolerance for substitution of residues within the membrane [25] compared to those within loop sequences.

Except for recovery from inactivation, the SLEN substitution did not seem to alter the properties of μ1 channels in HEK293 cells. A recent study suggested that the S3–S4 linker might be a determinant of activation kinetics of the potassium channel α-subunit [32]. Our data indicate that the D4S3–S4 linker does not play the same role in sodium channels. It remains unclear what causes the markedly slower kinetics in the TTX-R current and SNS recombinant channels. Because of the high degree of conservation of D4S1–S6 sequences, it is unlikely that these regions are responsible for the difference. The D3–4 linker, which has been implicated as the inactivation particle, is also highly conserved between SNS and other sodium channel isoforms. It is possible that the SLEN sequence in the SNS subunit interacts with other sequences in the native channel to slow down the movement of S4 in the membrane, thus impacting the kinetic properties of the current. Although the SLEN substitution is not sufficient to induce the dramatic changes in gating kinetics or voltage dependence that are observed with SNS channels, it appears to contribute to rapid repriming in these channels.

Acknowledgements: This work was supported in part by grants from the National Multiple Sclerosis Society, the Medical Research Service, Department of Veterans Affairs. We thank B.R. Toftness for technical assistance.

References

[1] Hille, B. (1992) Ionic Channels of Excitable Membranes, Sinauer, Sunderland, MA.
[2] Isom, L.L., De Jongh, K.S. and Catterall, W.A. (1994) Neuron 12, 1183–1194.
[3] West, J.W., Patton, D.E., Scheuer, T., Wang, Y., Goldin, A.L. and Catterall, W.A. (1992) Proc. Natl. Acad. Sci. USA 89, 10910–10914.

[4] Eaholtz, G., Scheuer, T. and Catterall, W.A. (1994) Neuron 12, 1041–1048.
[5] Fozzard, H.A. and Hanck, D.A. (1996) Physiol. Rev. 76, 887–926.
[6] Goldin, A.L. (1995) in: Handbook of Receptors and Channels (North, R.A., Ed.), pp. 73–100, CRC press, Boca Raton, FL.
[7] Mannuzzu, L.M., Moronne, M.M. and Isacoff, E.Y. (1996) Science 271, 213–216.
[8] Yang, N., George Jr., A.L. and Horn, R. (1996) Neuron 16, 113–122.
[9] Trimmer, J.S. et al. (1989) Neuron 3, 33–49.
[10] Ukomadu, C., Zhou, J., Sigworth, F.J. and Agnew, W.S. (1992) Neuron 8, 663–676.
[11] George, A.L., Komisarof, R.G., Kallen, R.G. and Barchi, R.L. (1992) Ann. Neurol. 31, 131–137.
[12] Wang, D.W., George Jr., A.L. and Bennett, P.B. (1996) Biophys. J. 70, 238–245.
[13] Akopian, A.N., Sivilotti, L. and Wood, J.N. (1996) Nature 379, 257–262.
[14] Sangameswaran, L. et al. (1996) J. Biol. Chem. 271, 5953–5956.
[15] Dib-Hajj, S., Black, J.A., Felts, P. and Waxman, S.G. (1996) Proc. Natl. Acad. Sci. USA 93, 14950–14954.
[16] Cummins, T.R. and Waxman, S.G. (1997) J. Neurosci. 17, 3503–3514.
[17] Catterall, W.A. (1995) Annu. Rev. Biochem. 64, 493–531.
[18] Sangameswaran, L. et al. (1996) J. Biol. Chem. 271, 5953–5956.
[19] Kostyuk, P.G., Veselovsky, N.S. and Tsyndrenko, A.Y. (1981) Neuroscience 6, 2423–2430.
[20] Caffrey, J.M., Eng, D.L., Black, J.A., Waxman, S.G. and Kocsis, J.D. (1992) Brain Res. 592, 283–297.
[21] Elliott, A.A. and Elliott, J.R. (1993) J. Physiol. 463, 39–56.
[22] Chahine, M., George Jr., A.L., Zhou, M., Ji, S., Sun, W., Barchi, R.L. and Horn, R. (1994) Neuron 12, 281–294.
[23] Rogers, J.C., Qu, Y., Tanada, T.N., Scheuer, T. and Catterall, W.A. (1996) J. Biol. Chem. 271, 15950–15962.
[24] Yang, N., Ji, S., Zhou, M., Ptacek, L.J., Barchi, R.L., Horn, R. and George Jr., A.L. (1994) Proc. Natl. Acad. Sci. USA 91, 12785–12789.
[25] Ji, S., George Jr., A.L., Horn, R. and Barchi, R.L. (1996) J. Gen. Physiol. 107, 183–194.
[26] Dib-Hajj, S.D., Hinson, A.W., Black, J.A. and Waxman, S.G. (1996) FEBS Lett. 384, 78–82.
[27] Horton, R.M., Ho, S.N., Pullen, J.K., Hunt, H.D., Cai, Z. and Pease, L.R. (1993) Methods Enzymol. 217, 270–279.
[28] Felipe, A., Knittle, T.J., Doyle, K.L. and Tamkun, M.M. (1994) J. Biol. Chem. 269, 30125–30131.
[29] George Jr., A.L., Knittle, T.J. and Tamkun, M.M. (1992) Proc. Natl. Acad. Sci. USA 89, 4893–4897.
[30] Akopian, A.N., Souslova, V., Sivilotti, L. and Wood, J.N. (1997) FEBS Lett. 400, 183–187.
[31] Roy, M.L. and Narahashi, T. (1992) J. Neurosci. 12, 2104–2111.
[32] Mathur, R., Zheng, J., Yan, Y. and Sigworth, F.J. (1997) J. Gen. Physiol. 109, 191–199.